A model to predict saturated critical heat flux in minichannels and microchannels

Ali Koşar

Mechatronics Engineering Program, Sabancı University, Tuzla, Istanbul 34956, Turkey

Abstract

A new model to predict saturated critical heat flux (CHF) conditions in minichannels and microchannels was developed. The model was compared to 151 experimental data points obtained from CHF studies on mini- and microchannels encompassing various working fluids (Water, R-123, R-113, R-134a, and R-245fa) over a broad range of mass velocities (50–1600 kg/m^2 s) and pressures (101–888 kPa). A strong correlation between the model and experimental data was supported by an overall mean absolute error (MAE) of 25.8%. Better predictions were noted (MAE = 21.3%) for experiments carried out using thin wall/substrate minichannel and microchannel configurations as well as those configurations which were not vulnerable to boiling instabilities. The consistent performance and broad applicability of this model demonstrate it as a viable tool for predicting the CHF in minichannels and microchannels.

Keywords: Critical heat flux; Saturated convective boiling; Microchannels; Minichannels; Boiling instabilities

1. Introduction

Heat dissipation from high power microelectronic devices continues to pose stringent challenges due to their increased functionality and demands. New cooling technologies are urgently sought to address the need to effectively dissipate heat, so that more compact and functional devices can be realized. Flow boiling is considered superior to single-phase flow since higher power densities can be achieved for a fixed mass velocity while featuring a comparatively lower surface temperature rise. The most limiting factor in boiling flow systems is known as the critical heat flux (CHF) condition, which imposes an upper limit on the heat flux applied to microchannel surface.

Under saturated boiling conditions, the CHF condition is associated with the dryout of the liquid film along the channel wall. At CHF condition, a sudden permanent dryout condition on heated microchannel surfaces accompanied by a severe surface temperature rise, which leads to the burnout of microchannel surfaces.

E-mail address: kosara@sabanciuniv.edu.

A large number of CHF prediction methods such as Bowring [1], Katto and Ohno [2], and Shah [3] have been developed for dryout type CHF based on empirical correlations, while there also exist semi-analytical and analytical models such as Whalley et al. [4], Govan et al. [5], and Revellin and Thome [6]. That being said, predicting the CHF using these methods is very cumbersome. Many lookup tables or charts developed for different working fluids at different parameter ranges must be cross-checked at different conditions when using some prediction methods. Similarly, complex nonlinear systems of differential equations must be solved to compute the CHF in utilizing semi-empirical models. Thus, it would appear that a practical prediction method is lacking to simultaneously predict dryout type CHF conditions of various working fluids over a large range of operating conditions, and to correlate existing experimental CHF data within acceptable limits. Such a claim is not necessarily unfounded, particularly in view that such predictions strongly depend on the microchannel configuration and operating conditions and thus, these models cannot supply any consistent prediction capability over a broad range of application.

In recent studies, research has been directed to investigate critical heat flux in minichannels and microchannels [6–15]. As

Nomenclature

C	liquid droplet concentration	$kg\,m^{-3}$
c_p	specific heat at constant pressure	$kJ\,kg^{-1}\,°C^{-1}$
d_h	channel hydraulic diameter	m
e	liquid droplet quality	
f	liquid film quality	
G	mass velocity based on the entire cross sectional area	$kg\,m^{-2}\,s^{-1}$
h_{FG}	latent heat of vaporization	$J\,kg^{-1}$
k_d	deposition mass transfer coefficient	$m\,s^{-1}$
L	channel length	m
L_h	heated channel length	m
$\dot{m}$	mass flow rate	$kg\,s^{-1}$
$\dot{m}_e$	mass flow rate of liquid droplets	$kg\,s^{-1}$
$\dot{m}_f$	mass flow rate of liquid film	$kg\,s^{-1}$
$\dot{m}_v$	mass flow rate of vapor core	$kg\,s^{-1}$
M_t	total number of data points	
MAE	mean absolute error	
P_c	perimeter of the vapor core	m
P_{ch}	perimeter of the channel cross sectional area	m
p	pressure	kPa
Pr	Prandtl number	
q''	heat flux based on the heat transfer surface area of the channel	$W\,cm^{-2}$
T	temperature	°C
U	the parameter under investigation	
W	channel width	m
x	mass quality	
x_e	exit mass quality	
z	distance from inlet	m

Greek

Γ_d	deposition mass transfer rate per unit channel length	$kg\,m^{-1}\,s^{-1}$
Γ_{FG}	evaporation mass transfer rate per unit channel length	$kg\,m^{-1}\,s^{-1}$
μ	viscosity	$kg\,m^{-1}\,s^{-1}$
υ	specific volume	$m^3\,kg^{-1}$
ρ	density	$kg\,m^{-3}$

Subscript

av	average
ch	channel
CHF	critical heat flux
cr	critical
e	exit
F	fluid
G	gas
i	inlet
j	index in Eq. (8)
L	liquid
SAT	saturation
sub	subcooled

a result of those studies, several refined correlations and prediction methods have been proposed. However, only a limited number of data points (in most cases only the data obtained by the same authors) was taken into consideration while testing or developing the prediction method in empirical [7–14] and analytical [6,15] approaches. Currently, a general and useful prediction method based on the physics of flow boiling is sought to correlate existing CHF data and predict the CHF over broad operating conditions. In this article, a practical model to predict the CHF in minichannels and microchannels will be introduced and its performance will be assessed using the existing CHF data from prior studies.

2. Model

In this model a dryout type CHF condition (also known as saturated CHF) is assumed. According to previous studies, three different flow patterns are distinguishable at high heat fluxes [12,13]. Bubbly flow consisting of small bubbles emerging from the channel wall occupies the inlet region (Fig. 1). These bubbles gradually enlarge in departing from the inlet. At a certain point, a growing bubble occupies the entire cross section of the channel of the channel and is then pushed by the drag force induced by the flow. As a result, the resultant big slug breaks down while moving along the channel, so that a two-phase mixture is established and starts to propagate. This two-phase mixture transforms toward the exit region into a spray-annular flow pattern, which is characterized by a liquid film along the channel walls and a vapor core with entrained liquid sprays. The liquid layer grows thinner and thinner along the channel with increasing heat flux. At a certain heat flux threshold, the liquid layer completely evaporates at the exit (Fig. 1b), and a permanent dry spot forms, which gives rise to a sharp local temperature rise, thereby triggering the CHF condition. The corresponding heat flux required to reach this critical condition at the exit is considered to be the CHF of this model.

The total mass flow rate across the cross section may be expressed as the sum of three components of spray-annular flow, namely, the flow rates of the liquid droplets, liquid film, and vapor core:

$$\dot{m} = \dot{m}_e + \dot{m}_f + \dot{m}_v \tag{1}$$

The above equation can be rearranged in terms of ratios of each component to express the total mass flow rate:

$$e + f + x = 1 \tag{2}$$

where e, f, and x depict the liquid droplet quality, liquid film quality, and mass quality, respectively. At the location of the dryout f becomes zero, and the derivative of the mass velocity fraction of liquid film as a function of location, which is also the difference between deposition and evaporation mass transfer rates, will become also zero:

$$\frac{d\dot{m}_f}{dz} = 0 = -\Gamma_{FG} + \Gamma_d \tag{3}$$

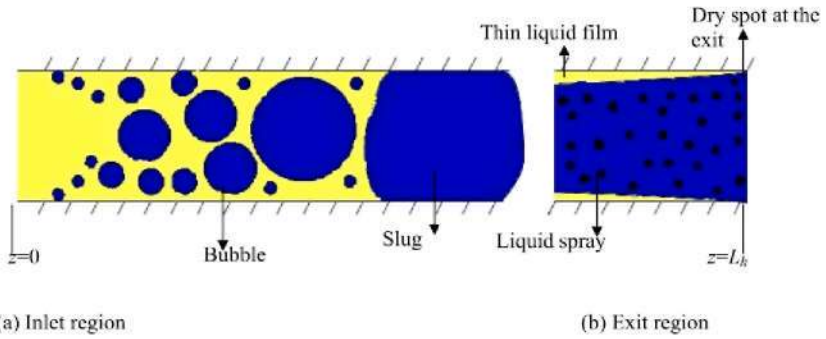

Fig. 1. Flow patterns depicted along the micro channel at high heat flux: (a) Inlet region (bubbly and slug flow patterns). (b) Exit region (spray-annular flow pattern with dryout condition at $z = L_h$).

where $\Gamma_{\rm FG}$ and Γ_d are evaporation mass transfer rate per unit channel length and deposition mass transfer rate per unit channel length. Evaporation mass transfer rate per unit channel length is defined as:

$$\Gamma_{\rm FG} = \frac{q''_{\rm CHF} P_{\rm ch}}{h_{\rm FG}} \tag{4}$$

The deposition mass transfer rate per unit channel length is related to the deposition mass transfer coefficient k_d, vapor core perimeter P_c, and liquid droplet concentration C, according to the following expression:

$$\Gamma_d = P_c k_d C \tag{5}$$

where $C = e/(x\upsilon_G + e\upsilon_F)$ and at the dryout location $P_c = P_{\rm ch}$.

At the CHF condition, the liquid film dries out, so that there is only vapor phase with liquid droplets ($x = x_{\rm cr}$, $e + x_{\rm cr} = 1$), and C becomes:

$$C = \frac{1 - x_{\rm cr}}{x_{\rm cr}\upsilon_G + (1 - x_{\rm cr})\upsilon_F} \tag{6}$$

where υ_F and υ_G are the liquid and vapor phase specific volumes.

Critical heat flux is triggered at the exit, when the liquid annular film either completely evaporates or entrains from the surface. At this condition, the critical quality is equal to the exit quality, which is expressed as:

$$x_{\rm cr} = x_e = \frac{q''_{\rm CHF} P_{\rm ch} L_h - \dot{m} c_p \Delta T_{\rm sub}}{\dot{m} h_{\rm FG}} \tag{7}$$

Eqs. (1)–(7) can be solved iteratively for critical heat flux and critical exit quality. In performing this analysis, it is vital to pick an appropriate k_d expression. In the literature, it has been already emphasized that conventional scale correlations are not applicable at the microscale [16]. Patankar and Puranik [17] empirically found a constant value for the deposition mass transfer coefficient ($k_d = 15 \times 10^{-2}$ m/s) in microchannels, so that they could successfully represent the existing heat transfer data for annular flow in their numerical study. This constant value has also been used in the present study for the sake of simplicity, so that the critical heat flux could be predicted without relying on any empirically developed prediction methods or solving complex partial differential equations.

The mean absolute error (MAE) is used to compare the experimental results with the prediction of the model according to the following expression:

$$\text{MAE} = \frac{1}{M_t}\sum_{j=1}^{M_t} \frac{|U_{\rm exp} - U_{\rm theoretical}|}{U_{\rm exp}} 100\% \tag{8}$$

3. Results and discussion

3.1. General considerations

The model presented above was tested using experimental data of previous studies (listed in Table 1) on minichannels and microchannels, where dryout type CHF mechanism was reported. In most of the prior studies, the experimental data was explicitly displayed, whereas in others the experimental data was carefully extracted from the graphical illustrations. Wall/substrate thickness, channel material, and inlet restriction were included as parameters in Table 1, in addition to the working fluid, configuration, and geometry. Hundred and fifty-one data points in literature were compared with the predictions of the model.

The model assumes a constant heat flux boundary condition along the microchannel, which corresponds to a thin channel wall/substrate configuration. When the channel wall/substrate thickness is significantly greater than the channel hydraulic diameter, a constant heat flux boundary condition is no longer valid due to conjugate effects, as these effects will significantly impact the CHF [18,19]. Moreover, for very thick channels, local burnouts may not cause any structural failure in the channel configuration, so that the CHF value might have been inadvertently reported as being higher than the heat flux noted upon the first occurrence of permanent dryout, which again is considered to define the CHF condition in the model. Thus, the CHF data reported for channels with thick wall/substrate thickness have a potential to be larger than the predictions of the model.

Boiling instabilities are a vital issue in flow boiling and could lead to premature CHF. Excursive instabilities and parallel channel instabilities are two important modes of instabilities detected in minichannels and microchannels. Excursive instabilities could be removed with a throttle valve; however, a valve for each channel is needed to suppress parallel channel insta-

Table 1
Summary of experimental specifications used in previous studies on CHF in minichannels and microchannels

Study	Geometry	Operating conditions and working fluid	Inlet restriction, wall/substrate thickness and material
Lazarek and Black [7]	Circular, vertical, single channel, $d_h = 3.1$ mm	R-113, $p_e = 117$–410 kPa $G = 232$–740 kg/m^2 s	Throttle valve, $t_s = 0.4$ mm, Stainless Steel
Bowers and Mudawar [8]	Circular, parallel, $d_h = 0.51$–2.54 mm	R-113, $p \sim 139$ kPa $G = 50$–151 kg/m^2 s	One throttle valve for all channels, $t_s \sim 9.24$–13.2 mm, Copper
Roach et al. [9]	Circular $d_h = 1.17$–1.45 mm	Water, $p_e = 344$–1043 kPa $G = 248$–1037 kg/m^2 s	Throttle valve, $t_s \sim 1$ cm, Copper
Yu et al. [10]	Circular, single channel, $d_h = 2.98$ mm	Water, $p_e \sim 200$ kPa $G = 50$–200 kg/m^2 s	Throttle valve, $t_s = 1.78$ mm, Stainless Steel
Qu and Mudawar [11]	Rectangular, 21 parallel 215 × 821 μm channels	Water, $p_e \sim 113$ kPa $G = 86$–368 kg/m^2 s	One throttle valve for all channels, Copper
Koşar et al. [12]	Rectangular, 5 rectangular channels $d_h = 0.223$ mm	Water, $p_e = 1$ atm $G = 115$–389 kg/m^2 s	Inlet orifice for each channel, $t_s = 0.15$ mm, Silicon
Koşar and Peles [13]	5 parallel rectangular channels $d_h = 0.223$ mm, Convective boiling	R-123, $p_e = 227$–520 kPa $G = 291$–1118 kg/m^2 s	Inlet orifice for each channel, $t_s = 0.15$ mm, Silicon
Wojtan et al. [14]	Circular $d_h = 0.5$–0.8 mm	R-134a, 245fa, $p_e \sim 888$ kPa $G = 400$–1600 kg/m^2 s	Throttle valve, thin wall, Stainless Steel
Kuan and Kandlikar [15]	Rectangular, 6 rectangular 1.054 × 0.157 mm channels	R-123, $p_e = 1$ atm $G = 410$–534 kg/m^2 s	Yes, one for all channels, $t_s = 12.3$ mm, Copper

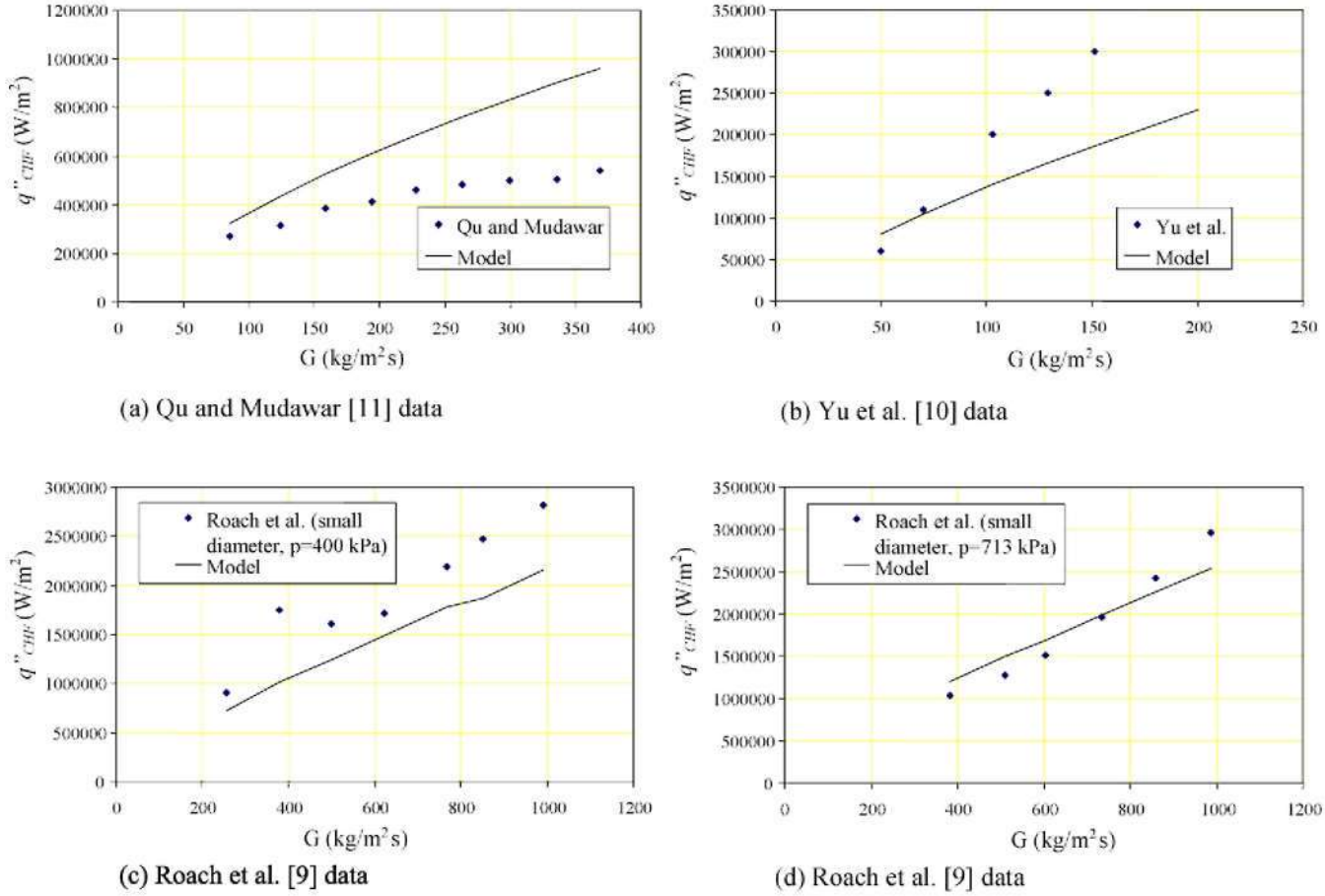

(a) Qu and Mudawar [11] data

(b) Yu et al. [10] data

(c) Roach et al. [9] data

(d) Roach et al. [9] data

Fig. 2.

bilities in multichannel arrangements [12,13,18,19]. The model assumes that there are neither excursive type nor parallel channel type instabilities and thus, it cannot take a premature CHF into account. As a result, the model has the potential of to over-predict experimental data obtained from configurations that are vulnerable to boiling instabilities and premature CHF.

Figs. 2–6 correlate experimental data in the literature against the predictions of the model. The model could predict all exper-

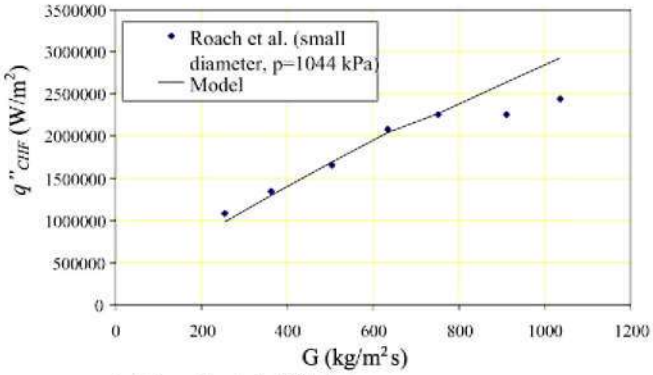

(e) Roach et al. [9] data

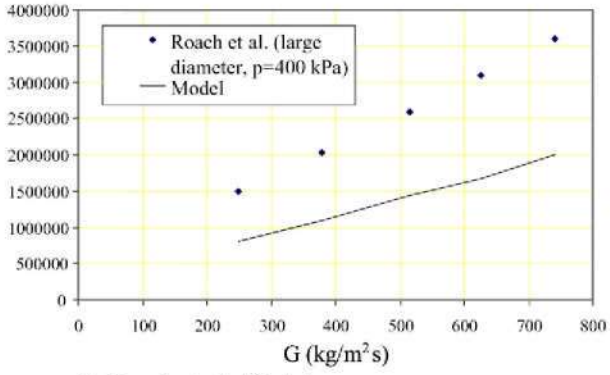

(f) Roach et al. [9] data

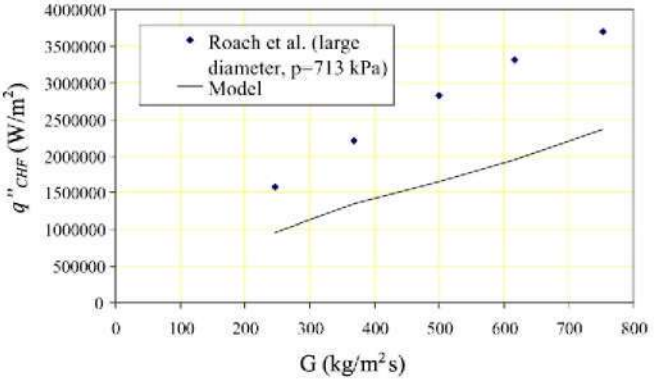

(g) Roach et al. [9] data

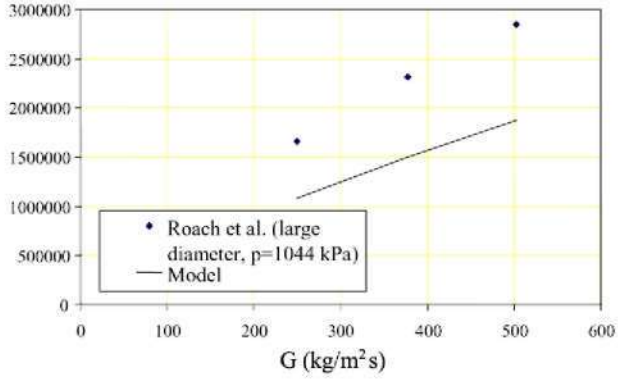

(h) Roach et al. [9] data

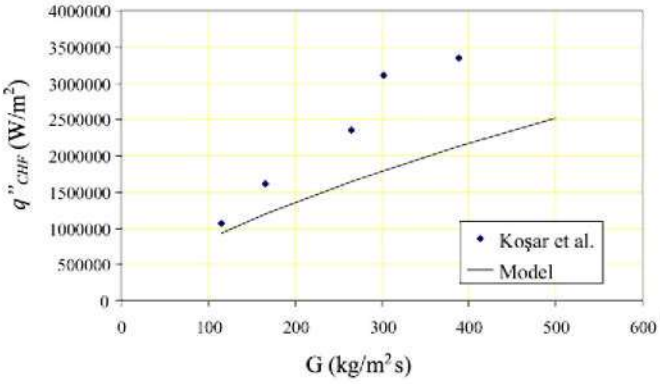

(i) Koşar et al. [12] data

Fig. 2. (*Continued*) Water CHF data compared against the predictions of the model.

imental data obtained in minichannels and microchannels with a MAE of 25.8%. More specifically, the MAEs were 28.9%, 18.2%, 28.2%, 26.0%, and 26.6%, and for water, R-123, R-113, R-134a and R-245fa, respectively. A discussion related to the model prediction capabilities is presented in the following sections.

3.2. *Predictions of CHF data with water as working fluid*

The predictions of water data by the model are displayed in Fig. 2. As can be seen from Fig. 2a, the model overpredicted all the Qu and Mudawar data [11]. In the study of Qu and Mudawar [11], it was reported that a throttle valve was used to suppress boiling instabilities for all the 21 channels. However, the existence of parallel channel instabilities could have significantly affected the CHF. The large number of parallel microchannels in their study could have mitigated this type of instabilities, so that early CHF could have occurred in this data set, which could explain the overprediction of the current model.

Although the data of Roach et al. [9] was well predicted by the model, most notable was the fact that most of their data was consistently underpredicted (Fig. 2 e–f). This underprediction might be due to the thick channel wall in their study. In a thick wall condition, the temperature distribution would be more uniform, thereby delaying the CHF condition. Moreover, the burnout condition at a certain location with a thick channel wall would not lead to catastrophic failure in this study. The discrepancy could also be associated with the fact that their

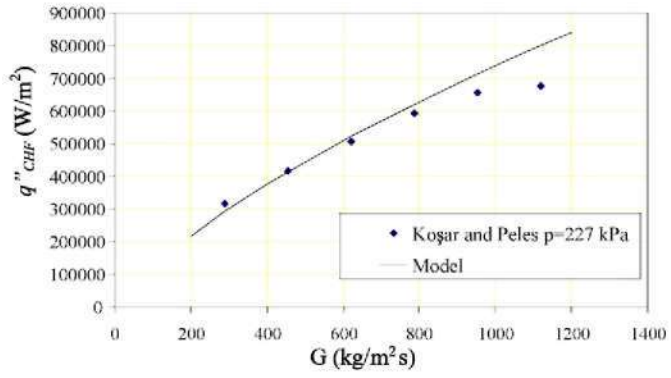

(a) Koşar and Peles [13] data

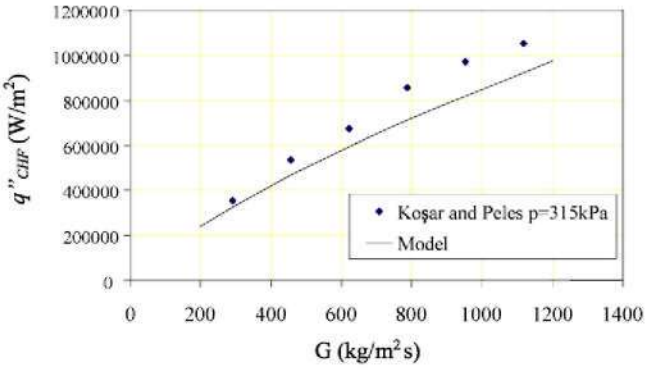

(b) Koşar and Peles [13] data

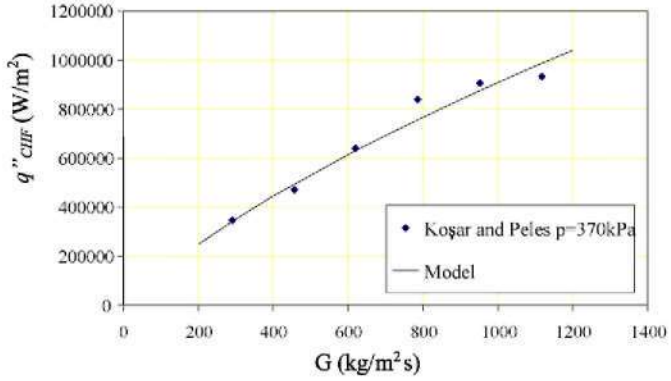

(c) Koşar and Peles [13] data

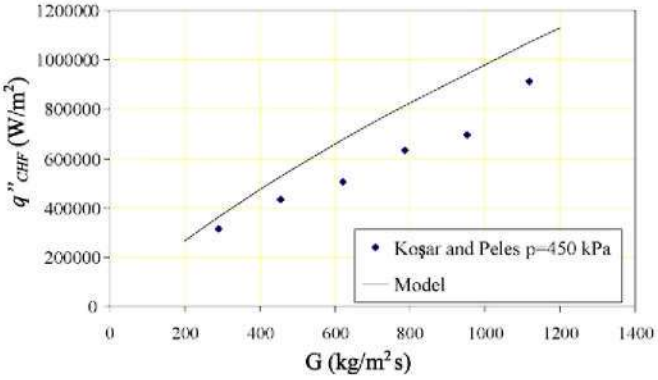

(d) Koşar and Peles [13] data

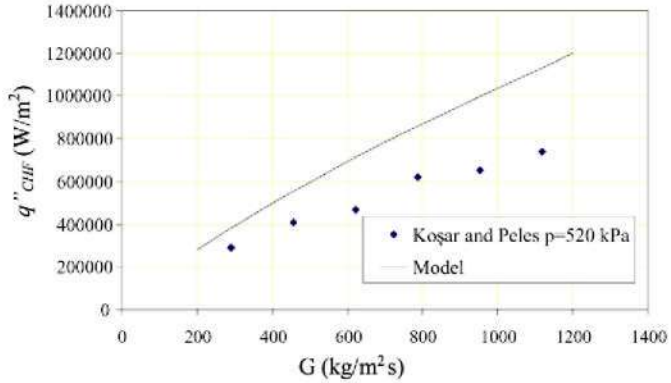

(e) Koşar and Peles [13] data

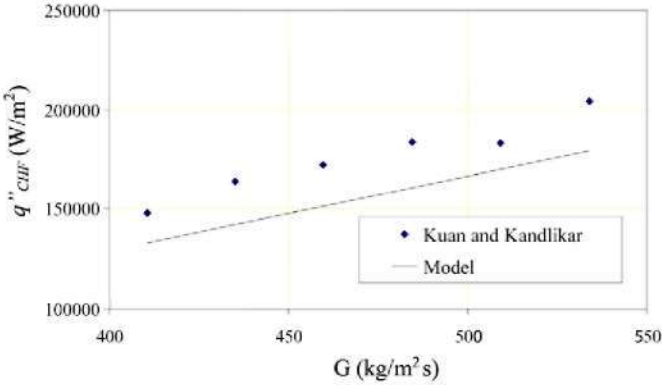

(f) Kuan and Kandlikar [15] data

Fig. 3. R-123 CHF data compared against the predictions of the model.

channel could withstand heat fluxes producing exit qualities even greater than one, a scenario that was indeed supported by some of their data.

Most of the CHF data of Yu et al. [10] and Koşar et al. [12] were underpredicted by the model, but the model still yielded a fair prediction. The model could not produce as good a prediction as R-123 for water. This indicated the complex contribution of working fluid effects on the CHF. As a result of change in the working fluid, the surface tension, the latent heat of vaporization, and the liquid-to-vapor density ratio (ρ_L/ρ_G), which all have significant influences on CHF, are also changed. Thus, the effect of working fluid could not be independently isolated well.

3.3. Predictions of refrigerant data as working fluid

The R-123 data (Fig. 3) obtained by Kuan and Kandlikar [15] and Koşar and Peles [13] could be predicted better than in the case of other working fluids (MAE = 18.2%). This finding could be related to the thin substrate/wall thickness, which better matches the model's assumption. Moreover, both excursive and parallel channel instabilities were suppressed in these studies using inlet restrictors.

The predictions of R-113 data are displayed in Fig. 4. Lazarek and Black data [7] could be fairly predicted (MAE = 22.8%) despite the consistent tendency to underpredict. Even though the flow was upward in this study, gravitational effects

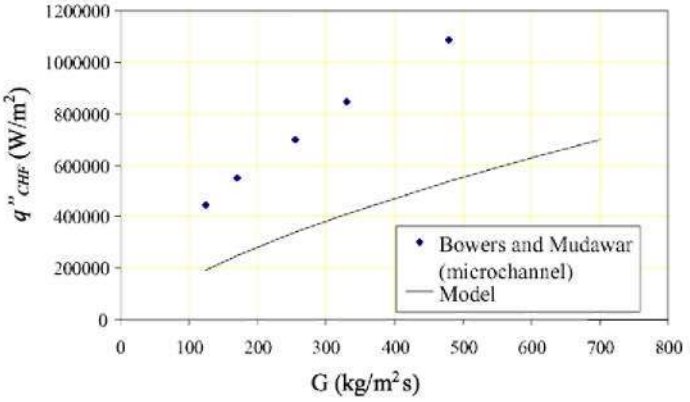

(a) Bowers and Mudawar [8] data (microchannel)

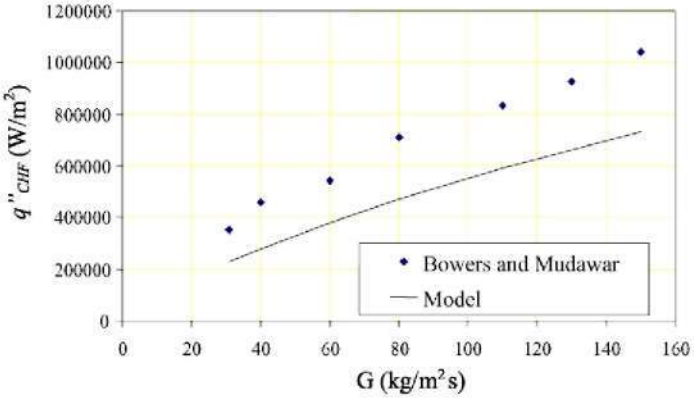

(b) Bowers and Mudawar [8] data (minichannel)

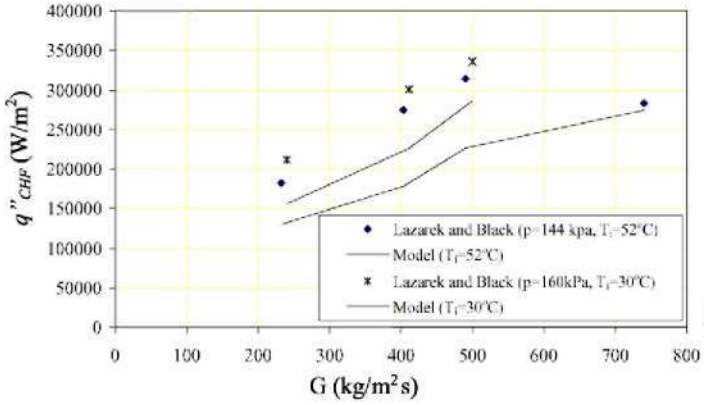

(c) Lazarek and Black [7] (minichannel)

Fig. 4. R-113 CHF data compared against the predictions of the model.

were assumed to be minor because of small channel size. The inlet restrictor, which was located at the inlet of the channel, suppressed boiling instabilities of thin wall channels. All these factors resulted in a fair prediction and the prediction was found to improve with increasing mass velocity.

All of Bowers and Mudawar data [8] was underpredicted by the model in a manner that was similar to the water data of Roach et al. [9]. Again, in Bowers and Mudawar [8] study, the substrate thickness is much greater than the channel size. A thick substrate thickness in this study increases the resistance of their heat sink to overheating due to permanent dry spots and delays the failure due to burnout to higher heat flux values.

From the work of Wojtan et al. [14], R-134a and R-245fa data are displayed along with the predictions of the model in Figs. 5 and 6. It can be observed that the model performs better with larger size channels in the case of R-134a (Fig. 5). Even though the predictions for smaller and larger size channels look similar for a specific mass velocity ($G = 500$ kg/m^2 s), the prediction for larger size channel is better over the entire mass velocity range. The MAE for the larger size channel is 24.2%, whereas the MAE of the smaller size channel is 31%. In the case of R-245fa data, the model results in a better prediction (MAE = 26.5%) compared to R-134a at the same mass velocity.

3.4. Overall performance of the model

The prediction capability of the model is displayed in Fig. 7. The majority of experimental data (65%) could be predicted within ±30%, while 91% of the data fell within ±50% of the experimental data. Overall, the prediction for thin wall channels with effective inlet restriction was much better. For such configurations [7,10,12,13], the MAE was 21.3% (Fig. 8). The findings indicate that the model is more appropriate for thin wall/substrate minichannels and microchannels having countermeasures against boiling instabilities. Its simplicity and performance would lend it amenable and desirable as a prediction tool for CHF in minichannels and microchannels.

3.5. Comparison with other prediction methods

Table 2 compares the prediction capability of the model against that of three previous prediction methods. Two methods (Shah [3] and Katto and Ohno [2] correlations) were general correlations to predict CHF in conventional size channels. The model of Revellin and Thome [6] was specifically developed to predict CHF in round microchannels.

It could be seen that the current model could predict the experimental data for each working fluid with a MAE less than 30%. Moreover, the prediction provided by other methods is clearly more sporadic than the current model. In particu-

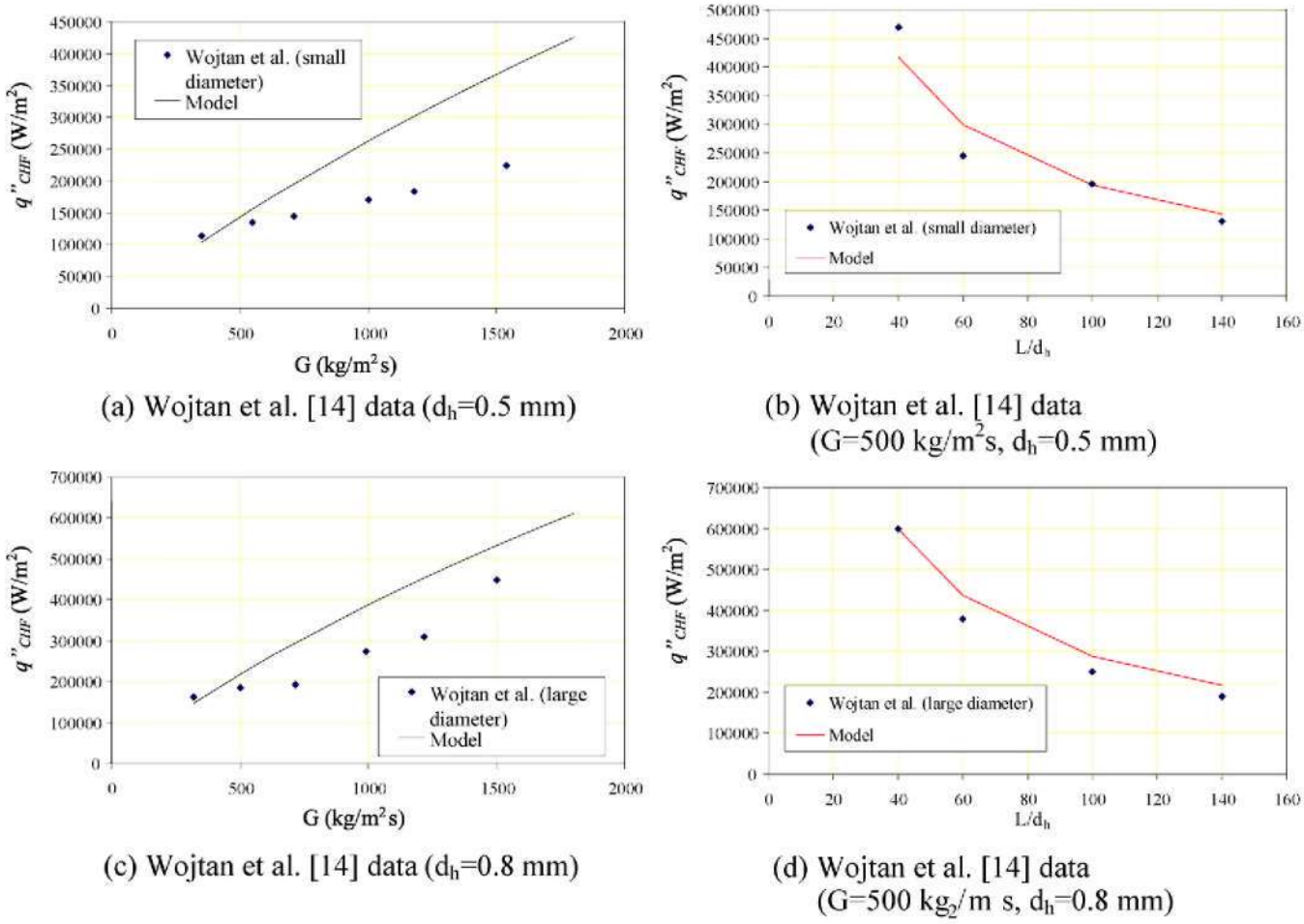

(a) Wojtan et al. [14] data (d_h=0.5 mm)

(b) Wojtan et al. [14] data (G=500 kg/m^{2}s, d_h=0.5 mm)

(c) Wojtan et al. [14] data (d_h=0.8 mm)

(d) Wojtan et al. [14] data (G=500 kg/m s, d_h=0.8 mm)

Fig. 5. R-134a CHF data compared against the predictions of the model.

Table 2
MAES (in %) obtained using available prediction methods as well as the current model

Study	Current method	Shah [3]	Revellin and Thome [6]	Katto and Ohno [2]
Wojtan et al. [14]	R-134a data 26	50.5	8	32.8
Wojtan et al. [14]	R-245f data 26.6	8.2		
Lazarek and Black [7]	R-113 data 28.2	43.8		114.5
Bowers and Mudawar [8]		97	15.4	41.2
Roach et al. [9]	Water data 28.9	25.4	Not included	37.5
Yu et al. [10]		28.2	Not included	17.7
Qu and Mudawar [11]		170.6	5.5	114.5
Koşar et al. [12]		17.4	N/A-rectangular	20.0
Koşar and Peles [13]	R-123 data 18.2	26.4	N/A-rectangular	24.7
Kuan and Kandlikar [15]		45.9	N/A-rectangular	38.5

lar, for some data points, the methods of Shah [3] and Katto and Ohno [2] result in a better prediction; however, for some other data points their predictions are poorer, which implies that the current method is more consistent in correlating the experimental data than these two methods. The model of Revellin and Thome [6] could provide a better prediction than the current model for round microchannel configurations. However, their model is much more complex than the current model. Moreover, it was applied to only one rectangular microchannel configuration and was not wholly validated for rectangular

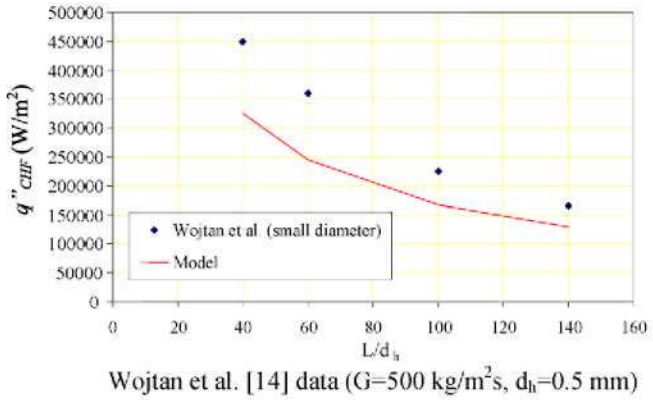

Fig. 6. R-245fa CHF data compared against the predictions of the model.

microchannels. The developers of this model proposed to extent their analysis to rectangular microchannels as future work.

Its simplicity, general applicability to round and rectangular microchannel geometries and consistent prediction capability with various working fluids presents the current model as a strong candidate to bridge the impasse in estimating the CHF in minichannels and microchannels.

4. Conclusions

A simple model has been developed to predict CHF in minichannels and microchannels. The experimental data in literature obtained from minichannels and microchannels of different sizes (0.223 mm < d_h < 3.1 mm) and shapes (circular and rectangular) under various operating conditions (mass ve-

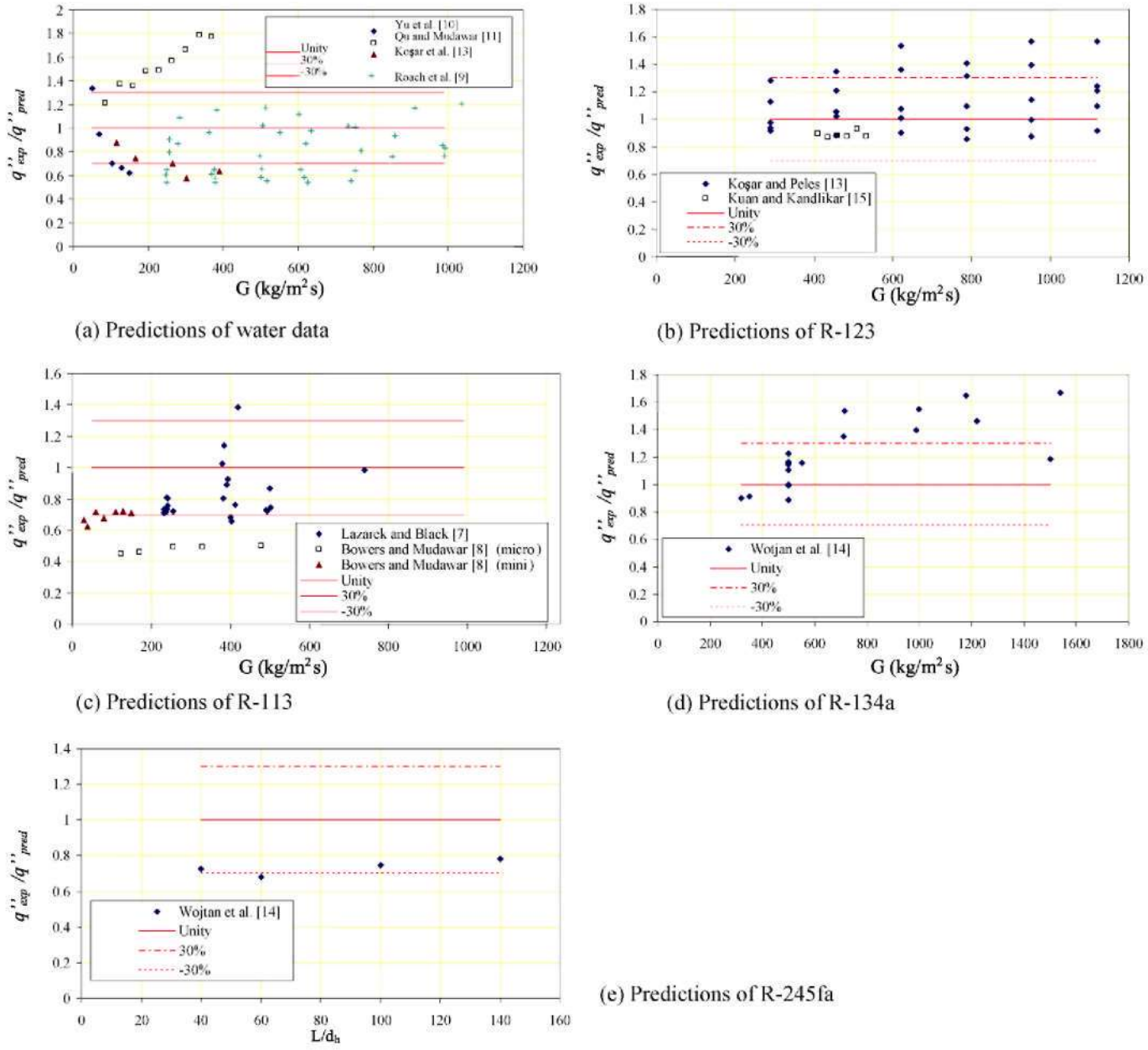

Fig. 7. Comparison of the model against experimental data obtained with different fluids.

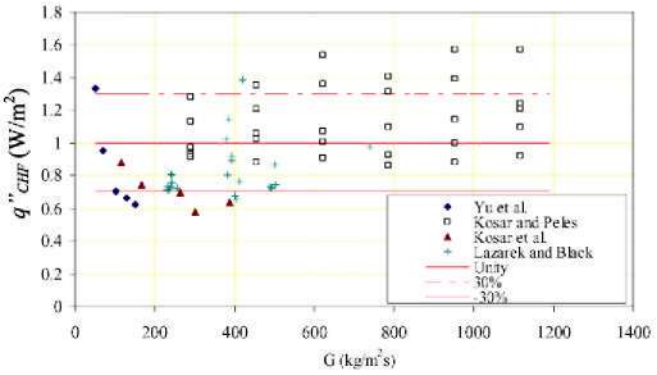

Fig. 8. Comparison of experimental data of Yu et al. [10], Koşar and Peles [13], Koşar et al. [12] and Lazarek and Black [7] against the model.

locities (50 kg/m^{2}s $< G <$ 1650 kg/m^{2}s, system pressures (101 kPa $< p <$ 888 kPa)), and working fluids (Water, R-123, R-113, R-134a, and R-245fa) were used to test the model. The model yielded a fair overall prediction over the entire range of experimental data. Its performance was consistently better for thin wall/substrate minichannel and microchannel configurations having effective protection from boiling instabilities.

The simplicity, consistent performance, and broad applicability of this model demonstrate it as a viable tool for predicting the CHF in minichannels and microchannels of various shapes under a broad range of working conditions.

Acknowledgements

The author is thankful to Prof. Alpay Taralp from material Science Engineering Program, Sabancı University for his valuable suggestions and comments.

References

[1] R.W. Bowring, A simple but accurate round tube uniform heat flux, dryout correlation over the pressure range 0.7–17 MN/m^2 (100–2500 psia), Br. Report AEEW-R 789, Winfrith, U.K., 1972.

[2] Y. Katto, H. Ohno, An improved version of the generalized correlation of critical heat flux for convection boiling in uniformly heated vertical tubes, International Journal of Heat and Mass Transfer 27 (9) (1984) 1641–1648.

[3] M.M. Shah, Improved general correlation for critical heat flux during upflow in uniformly heated vertical tubes, Heat and Fluid Flow 8 (4) (1987) 326–335.

[4] P.B. Whalley, P. Hutchinson, G.F. Hewitt, Calculation of critical heat flux in forced convective boiling, in: Proceedings of 5th International Heat Transfer Conference, Tokyo, Paper B6.11, 1974.

[5] A.H. Govan, G.F. Hewitt, D.G. Owen, T.R. Bott, An improved CHF modeling code, in: Proceedings of 2nd U.K. Conference on Heat Transfer, vol. 1, Institute of Mechanical Engineers, London, 1988, pp. 33–48.

[6] R. Revellin, J.R. Thome, A theoretical model for the prediction of the critical heat flux CHF in heated microchannels, International Journal of Heat and Mass Transfer 51 (5–6) (2008) 1216–1225.

[7] G.M. Lazarek, S.H. Black, Evaporative heat transfer, pressure drop and critical heat flux in a small vertical tube with R-113, International Journal of Heat and Mass Transfer 25 (7) (1982) 945–960.

[8] M.B. Bowers, I. Mudawar, High flux boiling in low flow rate, low pressure drop mini-channel and micro-channel heat sinks, International Journal of Heat and Mass Transfer 37 (2) (1994) 321–334.

[9] G.M. Roach, S.I. Abdel-Khalik, S.M. Ghiaasiaan, M.F. Dowling, S.M. Jeter, Low-flow critical heat flux in heated microchannels, Nuclear Science and Engineering 131 (3) (1999) 411–425.

[10] W. Yu, D.M. France, M.W. Wambsganns, J.R. Hull, Two-phase pressure drop, boiling heat transfer, and critical heat flux to water in a small-diameter horizontal tube, International Journal of Multiphase Flow 28 (2002) 927–941.

[11] W. Qu, I. Mudawar, Measurement and correlation of critical heat flux in two-phase micro-channel heat sinks, International Journal of Heat and Mass Transfer 47 (2004) 5749–5763.

[12] A. Koşar, C.J. Kuo, Y. Peles, Suppression of boiling flow oscillations in parallel microchannels by inlet restrictors, Journal of Heat Transfer 128 (2006) 251–260.

[13] A. Koşar, Y. Peles, Critical heat flux of R-123 in silicon-based microchannels, Journal of Heat Transfer 129 (7) (2007) 844–851.

[14] L. Wojtan, R. Revellin, J.R. Thome, Investigation of saturated critical heat flux in a single, uniformly heated microchannel, Experimental and Fluid Science 30 (8) (2006) 765–774.

[15] W.K. Kuan, S.G. Kandlikar, Experimental study on saturated flow boiling critical heat flux in microchannels, in: Proceedings of the Fourth International Conference on Nanochannels, Microchannels, and Minichannels, Limerick, Ireland, 2006, ICNMM2006-96044.

[16] W. Qu, I. Mudawar, Flow boiling heat transfer in two-phase micro-channel heat sink—I. Experimental investigation and assessment of correlation methods, International Journal of Heat and Mass Transfer 46 (15) (2003) 2755–2771.

[17] U. Patankar, B. Puranik, Modifications and extensions to the annular flow model, in: Proceedings of the Fourth International Conference on Nanochannels, Microchannels, and Minichannels, Limerick, Ireland, 2006, ICNMM2006-96053.

[18] A.E. Bergles, S.G. Kandlikar, Critical heat flux in microchannels: experimental issues and guidelines for measurement, in: Proceedings of the First International Conference on Microchannels, and Minichannels, Rochester, New York, 2003, ICMM2003-1016.

[19] A.E. Bergles, S.G. Kandlikar, On the nature of critical heat flux in microchannels, Journal of Heat Transfer 127 (2005) 101–107.